Relationship between ENSO and Rainfall in the Central Plain of Thailand

Chaweewan Wikarmpapraharn and Ekasit Kositsakulchai*

ABSTRACT

In this study, the response of monthly rainfall to the El Nino-southern oscillation (ENSO) was investigated by correlation analysis to determine the pattern and magnitude of the relationship, using rainfall datasets at four weather stations in the Central Plain of Thailand (Kanchanaburi, Lop Buri, Nakhon Sawan, Suphan Buri). The rainfall data sets characterized by the standardized precipitation index (SPI) and the strengths of ENSO characterized by the multivariate ENSO index (MEI) were searched to get the best SPI-MEI subsets by step-wise multiple regression. Six SPI time scales: 1-, 2-, 3-, 4-, 5-, and 6-months were chosen to form regression equations. The results indicated that the chosen statistical approach produced models that could be used to forecast SPI at least one fortnight ahead at 10% significance levels. It can be concluded from this study that the proposed models could contribute to irrigation water management and preparedness for water allocation planning during the dry period from November to April. However, regional synthesis of the equations is necessary in order to apply the proposed model on a regional scale.

Keywords: multivariate ENSO index (MEI), standardized precipitation index (SPI), El Nino southern oscillation (ENSO), rainfall, the central plain of Thailand.

INTRODUCTION

Rain water is a major factor in the planning and management of irrigation projects. Furthermore, it is an essential resource for agricultural water supply in Thailand. Paddy cultivation, one of the most weather-dependent sectors of all human activities, requires higher water consumption compared to other crops. Annual variation of rainfall coupled with inadequate storage leads to ineffectiveness and inaccuracy in the planning of irrigation projects and thus has a recognized impact on the country's economy, since rice is one of the most important crops for domestic consumption and export. Therefore, it is important to know whether or not there is a reduction in rain water quantity, since this information is useful for water management and preparedness, specifically during the dry post-rainy period.

Rainfall variation and uncertainty are believed to be related to a large scale ENSO phenomenon that is defined as the combination of ocean warming and the reversal of surface air pressure, at opposite ends of the tropical Pacific Ocean that usually occur simultaneously (Peskan,

Department of Irrigation Engineering, Faculty of Engineering at Kamphaeng Saen, Kasetsart University, Kamphaeng Saen Campus, Nakhon Pathom 73140, Thailand.
* Corresponding author, e-mail: fengesk@ku.ac.th

2001). In considering a number of studies and analyses that have been carried out so far, the general type of relationship and degree of association between rainfall over Thailand and ENSO is still ambiguous and cannot be pinpointed exactly. The analyses sometimes revealed different conclusions. For example, Xu *et al.* (2004) found a strong relationship existing between ENSO and rainfall in the Mae Klong and Ping River Basins, while Singhrattna *et al.* (2005) showed a significant relationship among those variables during the post-1980 period. In contrast, Otarig (2000) reported that there was no correlation between El Nino and rainfall over Thailand. The different results may be due to the large spatial and temporal variation of monsoon rains. Moreover, ENSO itself is a complex system, comprising several dynamic natural behavioral characteristics with tele-connections with local rainfall in many places around the globe. Thus, it becomes difficult to identify any single uniform relationship between ENSO and monsoon rainfall that holds up for different locations in Thailand. However, further analysis and research are still required to pursue the answers to these questions. Therefore, this research objective was to select the subsets of the ENSO index (MEI) and rainfall index (SPI) with the most potential to estimate rice water requirements during the post-rainy period by a crop growth model and provide a decision basis for water release scheduling at the paddy field level in the Central Plain of Thailand.

MATERIALS AND METHODS

Study area

Four rainfall stations were selected as representative of the study area: 1) Kanchanaburi, located near the western boundary of the central region (14° 01′ N, 99° 32′ E, 28 m above sea level); 2) Lop Buri, located near the northern boundary of the central region (14° 482 N, 100° 372 E, 10 m above sea level); 3) Nakhon Sawan, located in the northernmost province of the central region (15°482 N, 100° 082 E, 34 m above sea level); and 4) Suphan Buri, located in the central region (14° 282 N, 100° 082 E, 7 m above sea level). All stations are in the Central Plain of Thailand, which is mainly dominated by rice growing areas. Rice production from this region is a most important part of the country's economy, as this region produces huge quantities of rice for both domestic consumption and export. Water, one of the key factors for rice cultivation activities, is sourced from four main rivers: the Chao Phraya, Pa Sak, Mae Klong and Tha Chin. These rivers pass through the Central Plain and supply water for irrigated and non-irrigated paddy fields.

Consequently, rainfall data in this region have been selected for the study. The data from the period 1951-2007 and compiled by The Thai Meteorological Department were screened statistically before undertaking correlation analysis. The verification followed methods proposed in Dahmen and Hall (1991). Initially, a graphical exploration of the data was used to observe rainfall time series behavior and then a test for the absence of a trend (Haan, 1977) was applied. Stability of variances and means (Buishand, 1982) were considered next, before testing for the absence of persistence (Box and Jenkins, 1976) by computing the first serial-correlation coefficients. All annual rainfall time series that passed the screening criteria thresholds are graphically illustrated in Figure 2. Geo-referencing of the stations, as well as a summary of the statistical properties of the annual rainfall data are presented in Table 1. It can be seen that the annual rainfall data from the representative stations ranged from 1,100 to 1,200 mm, with a standard deviation of 210-255 mm and a coefficient of variation range of 19-23%.

Multivariate ENSO index

Owing to the ENSO effect on climate variability over several parts of the globe, many
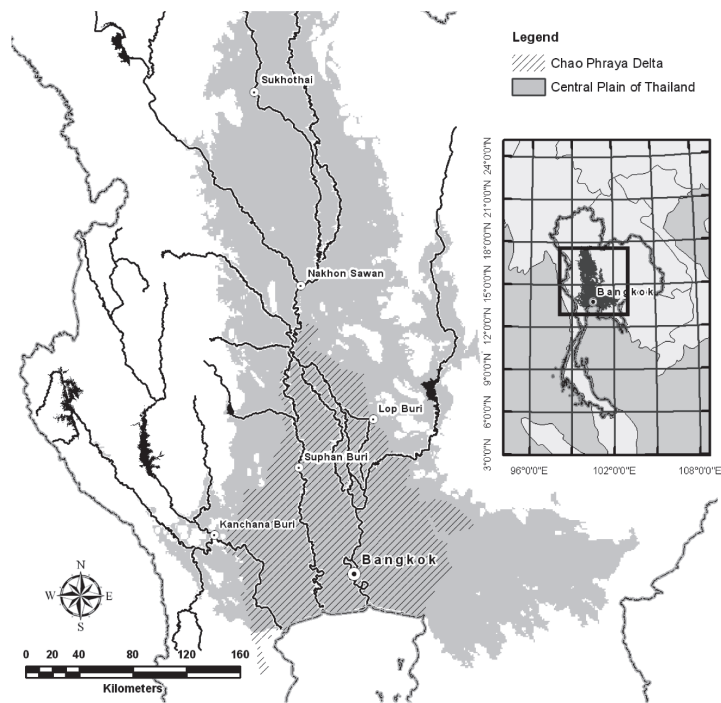
Figure 1 Locality map of the weather stations used in the study: Kanchanaburi (KA), Lop Buri (LB), Nakhon Sawan (NS), and Suphan Buri (SP).
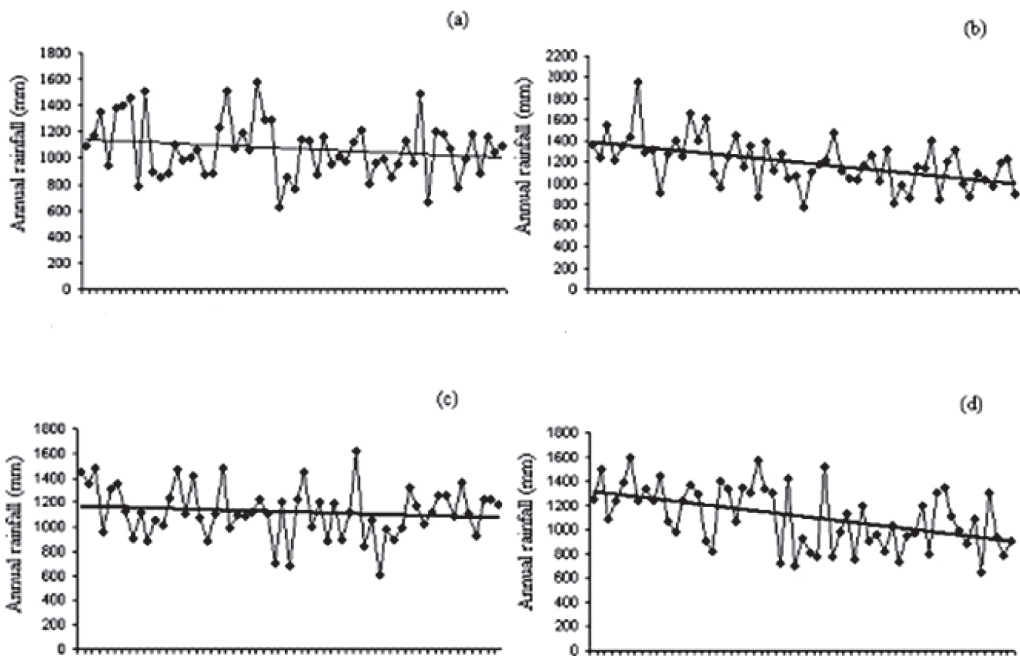

Figure 2 Annual rainfall time series at the weather stations (a) Kanchanaburi, (b) Lop Buri, (c) Nakhon Sawan and (d) Suphan Buri, from 1951-2007.

different indices have been developed to rate the severity and intensity of separate events over time. Nevertheless, there is currently no consensus within the scientific community as to which of the many indices best capture the ENSO phases (Hanley *et al*., 2003).

The multivariate ENSO index (MEI) is used to monitor and study the coupled oceanic-atmospheric character of ENSO, by basing its values on the principal variables observed over the tropical Pacific. MEI is defined as a weighted average of the six major features that approximate ENSO characteristics. These variables are: sea level pressure, sea surface temperature, surface air temperature, the east-west and north-south components of air surface wind, and the total amount of cloud. The MEI values shown in Figure 3 are a result of principal component analysis, which derives standard scores out of a large and variable databank. It is believed that because the variables are in large scale pattern forms, rather than point measurements, the variables can be used

Table 1 Weather station and basin names, period of data records, geo-reference of locations and statistical properties of annual rainfall at the study sites.

Stations	Basin names	Period of records	Geo-reference of locations			Statistical properties of annual rainfall		
			Lat.	Long.	Alt.	Mean	SD	CV
KA	Mae Klong	1951-2007	14° 01′	99° 32′	28	1073.83	217.61	0.20
LB	Pasak	1951-2007	14° 48′	100° 37′	10	1192.65	228.28	0.19
NS	Chao Praya	1951-2007	15° 48′	100° 10′	34	1127.27	210.75	0.19
SP	Tha Chin	1951-2007	14° 28′	100° 08′	7	1106.10	253.97	0.23

Note: KA = Kanchanaburi weather station
      LB = Lop Buri weather station
      NS = Nakhon Sawan weather station
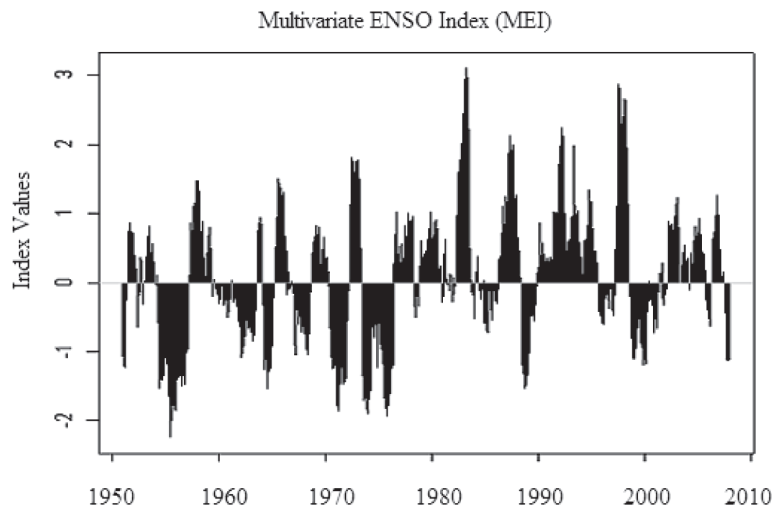   SP = Suphan Buri weather station

Figure 3 Time variation of ENSO events since 1950s, Positive and negative anomalies represent warm and cold events, respectively. ENSO index used is multivariate ENSO index (MEI) (Wolter and Timlin, 1993).

in relation to each other to obtain a more comprehensive measure of ENSO-related interactions (Wolter, 1999b). Research using MEI includes Shabbar *et al.* (1997), Wolter and Timlin (1993, 1998), Wolter (1999a, 1999b), Singh (2001), Peskan (2001) and Ortiz-Tancheza *et al.* (2002). These studies concentrated on the feasibility of the index and how it related to climatic phenomena in the areas of interest.

Standardized precipitation index

The standardized precipitation index (SPI) (McKee *et al.*, 1993) represents a Z-score or the number of standard deviations that an event deviates from the mean at a given time. Different time scales reflect the precipitation deficiency of the different segments of hydrological water resources, such as soil water, ground water and reservoir storage. The index is suitable for quantifying both dryness and wetness events. Studies using SPI and water resources availability include Lloyd-Hughes and Saunders (2002), Bordi *et al.* (2004), Vicente-Serrano (2006), and Cancelliere *et al.* (2007). SPI is calculated using the equations below.

The derivation of SPI (McKee *et al.*, 1993) begins with modeling the monthly precipitation time series using a gamma distribution, whose probability density function is defined by Equation 1:

$$g(x) = \frac{1}{\beta^{a}\Gamma(\alpha)}x^{\alpha-1}e^{-x/\beta}, \text{for } x > 0 \quad (1)$$

where: α is a shape parameter,
β is a scale parameter,
x is the amount of precipitation and
$\Gamma(\alpha)$ is the gamma function.

Fitting the distribution to the data requires α and β to be estimated, using approximation by means of a maximum-likelihood method for each station, for each time scale of interest and for each month of the year. Thus, Equation 2 is obtained:

$$\hat{\alpha} = \frac{1}{4A}\left(1+\sqrt{1+\frac{4A}{3}}\right), \hat{\beta} = \frac{\bar{x}}{\hat{\alpha}} \quad (2)$$

involving Equation 3:

$$A = \ln(\bar{x}) - \frac{\sum \ln(x)}{n} \quad (3)$$

where   n is the number of observations in which some precipitation has occurred for a given month and

$\bar{x}$ is the mean of the cumulative precipitation computed for the same month for the different years in the databank.

The resulting parameters are then used to find the cumulative probability of precipitation for a given month and time scale at the station considered. Substituting t with $x/\hat{\beta}$ produces the incomplete gamma-function (Equation 4):

$$G(x) = \int_{0}^{x} g(x)dx = \frac{1}{\hat{\beta}^{\hat{\alpha}}\Gamma(\hat{\alpha})}\int_{0}^{x} x^{\hat{\alpha}-1}e^{-x/\hat{\beta}}dx \quad (4)$$

Since the gamma-function is undefined for $x = 0$ and the precipitation field may contain zero values and $q = P(X = 0) > 0$ where $P(X = 0)$ is the probability of zero precipitation, the cumulative probability becomes Equation 5:

$$H(x) = q + (1 - q)G(x) \quad (5)$$

where, q is the probability of zero precipitation.

The cumulative probability distribution is then transformed into the standard normal distribution to yield the SPI (Equations 6-9):

$$Z = SPI = -\left(t - \frac{c_0 + c_1 t + c_2 t^2}{1 + d_1 t + d_2 t^2 + d_3 t^3}\right), \text{for } 0 < H(x) \leq 0.5 \quad (6)$$

$$Z = SPI = +\left(t - \frac{c_0 + c_1 t + c_2 t^2}{1 + d_1 t + d_2 t^2 + d_3 t^3}\right), \text{for } 0.5 < H(x) < 1.0 \quad (7)$$

$$t = \sqrt{\ln\left(t - \frac{1}{((H(x))^2}\right)}, \text{for } 0 < H(x) \leq 0.5 \quad (8)$$

$$t = \sqrt{\ln\left(t - \frac{1}{(1 - H(x))^2}\right)}, \text{for } 0.5 < H(x) < 1.0 \quad (9)$$

where $c_0, c_1, c_2, d_1, d_2,$ and d_3 are constants, with values $c_0 = 2.515517$, $c_1 = 0.802853$, $c_2 = 0.010328$, $d_1 = 1.432788$, $d_2 = 0.189269$, and $d_3 = 0.001308$.

Data

The data used in this study were the monthly rainfall data from the four study sites from 1951-2007 that had been screened as described above, and MEI data for the period 1951-2007 obtained from the NOAA-CIRES Climate Diagnostics Center, Boulder, U.S.A. MEI was used as the explanatory ENSO index in this study. Three other indices recorded during the same period were also taken from the same databank to observe their relationship. The indices chosen were two temperature-based indices, namely the oceanic Nino index (ONI) and the Japan Meteorological Agency index (JMA), and one pressure-based index, namely the southern oscillation index (SOI). The scatter plots in Figure 4 depict high correlation between MEI and the other indices, particularly between the temperature-based ONI and JMA indices. This supports the decision that MEI was appropriate enough to be used as the only input variable.
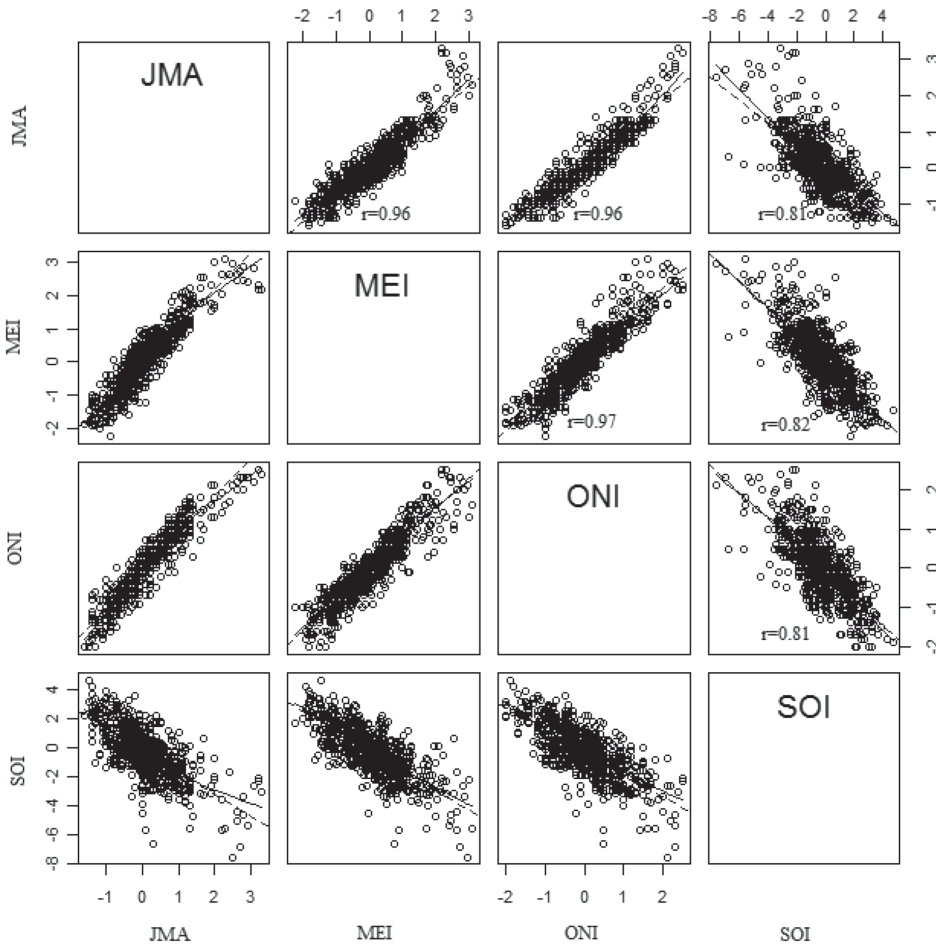

Figure 4 Correlation matrix between multivariate ENSO index (MEI), Japan Meteorological Agency index (JMA), oceanic nino index (ONI), and southern oscillation index (SOI) from 1951-2007.

Identification and manipulation of variables

The requirements for any useful predictor are firstly a good relationship with the selected SPI and secondly, a reasonable correlation and lead time (that is, months to season). For convenience, the year in which the MEI and SPI values were taken will be referred to as "year 0" and similarly "year -1" for the year prior to year 0 (Hong *et al.*, 2001). Time scales for the accumulation of rainfall in this study were defined in terms of the dry period after the rainy season from November to April. Therefore, six time scales of cumulative monthly rainfall data at each station were transformed into 1-, 2-, 3-, 4-, 5-, and 6-month SPI values with mean = 0 and standard deviation = 1. Those computed SPI values were denoted by SPI_Nov, SPI_Dec, SPI_Jan, SPI_Feb, SPI_Mar and SPI_Apr for 1-month cumulative rainfall, SPI_ON, SPI_ND, SPI_DJ, SPI_JF, SPI_FM and SPI_MA for 2-month cumulative rainfall, SPI_SON, SPI_OND, SPI_NDJ, SPI_DJF, SPI_JFM and SPI_FMA for 3-month cumulative rainfall, SPI_ASON, SPI_SOND, SPI_ONDJ, SPI_NDJF, SPI_DJFM and SPI_JFMA for 4-month cumulative rainfall, SPI_JASON, SPI_ASOND, SPI_SONDJ, SPI_ONDJF, SPI_NDJFM and SPI_DJFMA for 5-month SPI, and SPI_JJASON, SPI_JASOND, SPI_ASONDJ, SPI_SONDJF, SPI_ONDJFM and SPI_NDJFMA for 6-month SPI. The explanatory variables were twelve sliding bi-monthly values of MEI for Dec/Jan (MEI_DJ), Jan/ Feb (MEI_JF), Feb/Mar (MEI_FM), Mar/Apr (MEI_MA), Apr/ May (MEI_AM), May/Jun (MEI_MJ), Jun/Jul (MEI_JJ), Jul/Aug (MEI_JA), Aug/Sep (MEI_AS), Sep/Oct (MEI_SO), Oct/Nov (MEI_ON) and Nov/Dec (MEI_ND).

Correlation analysis and selection of variables

Traditional multiple linear regression involves fitting a linear function to a response variable (such as SPI) and independent variables (such as MEI). In this analysis, a multiple regression was chosen to model a quantitative

dependent variable Y through a linear combination of p quantitative explanatory variables X1, X2, Xp. The deterministic model for observation i (not taking randomness into account) is described by Equation 10:

$$Y_i = \beta_i + \sum_{j=1}^{p} \beta_j X_{ij} + \varepsilon_i \qquad (10)$$

where Y_i is the observed value for the dependent variable for observation i,

X_{ij} is the value taken by variable j for observation i,

β_i ,.., are estimated from the data, and

i is the error of the model, assumed to be normally distributed with mean 0 and variance σ_e^2.

The normalized MEI, with mean 0 and σ_e^2 were taken as covariates and SPI as the response variable in the applied regression Equation 11:

$$SPI_i = \beta_i + \sum_{j=1}^{p} \beta_{ij} MEI_{ij} + \varepsilon_i \qquad (11)$$

Parameters of significance in the prediction were selected by stepwise variable selection. This approach is a systemic method for adding and removing terms from a multi-linear model, based on their statistical significance in a regression, beginning with fitting an initial model and then comparing the explanatory power of incrementally larger and smaller models. At each step, the p-value of an F-statistic is computed to test models with and without a potential term. If a term is not currently in the model, the null hypothesis is that the term would have a zero coefficient if added to the model. If there is sufficient evidence to reject the null hypothesis, the term is added to the model. Conversely, if a term is currently in the model, the null hypothesis is that the term has a zero coefficient. If there is insufficient evidence to reject the null hypothesis, the term is removed from the model. However, once a variable is in the equation, it may be

swapped with a variable not in the equation or it may be removed from the equation all together.

The stepwise procedure was used for selecting subsets due to the fact that there is no theoretical basis for choosing the form of a model and no assessment of correlations among terms. Furthermore, the number of significant predictors is large if all combinations are considered. Consequently, it might be possible to include redundant terms in a model that could confuse the identification of significant effects.

Model evaluation

The models were verified in split-validated mode to see how well they performed. The data were split randomly into a 75% training sample and a 25% validation sample. The training sample was used to develop the model, while its effectiveness was evaluated on the validation sample to test the applicability of the model by applying it to data independent of the model development.

The validation was assumed to be successful if the training sample produced the same subset of predictors produced by the regression model of the full data set and the shrinkage (R^2 for the 75% training sample - R^2 for the 25% validation sample) was 5% (0.05) or less.

RESULTS

From the set of MEI and SPI predictors identified in the previous section, optimal subsets of the regression model were selected at the 10% significant level. Tables 2 to 5 present features of the SPI/MEI relationship at the Kanchanaburi, Lop Buri, Nakhon Sawan and Suphan Buri weather stations.

Table 2 Predictor selection for SPI of April by step-wise method at 10% significant level and regression equations of SPI and MEI at Kanchanaburi weather station.

SPI time scale	Start month	Regression equations
1-m	Apr (0)	SPI_Apr (0) = -0.127*MEI_ON (-1)*MEI_ND (-1) *MEI_DJ 0)
2-m	Mar (0)	SPI_MA (0) = -0.156*MEI_ON (-1)*MEI_ND (-1) *MEI_DJ (0)
3-m	Feb (0)	SPI_FMA (0) = -0.185*MEI_SO(-1)*MEI_ON (-1)*MEI_ND (-1)
4-m	Jan (0)	SPI_JFMA (0) = -0.174*MEI_AS(-1)*MEI_SO(-1)*MEI_ON (-1)
5-m	Dec (-1)	SPI_DJFMA (0) =-0.113*MEI_JJ(-1)*MEI_JA(-1)*MEI_AS(-1)
6-m	Nov(-1)	SPI_NDJFMA (0) = 0.115*MEI_FM(-1)*MEI_MA(-1)*MEI_JA(-1)*MEI_AS (-1)

Table 3 Predictor selection for SPI of April by step-wise method at 10% significant level and regression equations of SPI and MEI at Lop Buri weather station.

SPI time scales	Start month	Regression equation
1-m	Apr (0)	SPI_Apr (0) = -0.081* MEI_ON (-1)*MEI_ND (-1) *MEI_DJ (0)
2-m	Mar (0)	SPI_MA(0) = -0.128*MEI_ON (-1)*MEI_ND (-1) *MEI_DJ (0)
3-m	Feb (0)	SPI_FMA (0) = -0.139*MEI_SO(-1)*MEI_ON (-1)*MEI_ND (-1)
4-m	Jan (0)	SPI_JFMA (0) = -0.082*MEI_AS(-1)*MEI_SO(-1)*MEI_ON (-1)
5-m	Dec (-1)	SPI_DJFMA (0) =0.149*MEI_AM(-1)*MEI_MJ(-1)
6-m	Nov(-1)	SPI_NDJFMA (0) = 0.07*MEI_MA(-1)*MEI_MJ(-1)*MEI_JJ(-1)*MEI_JA(-1)

The SPI time scales over 1, 2, 3 and 4 months (SPI_Apr (0), SPI_MA (0), SPI_FMA (0) and SPI_JFMA (0)) at all stations are displayed in Tables 2 to 5, respectively. They were all correlated with the same ENSO strength and phases, that is the ENSO event during September in the previous year that lasted until January of the next year (MEI_AS (-1), MEI_SO (-1), MEI_ON (-1), MEI_ND (-1) and MEI_DJ (0). The 5- and 6- month SPI values were less specific in selecting the predictors. The MEI values chosen for SPI_DJFMA(0) ranged from one at Suphan Buri (Table 5), two at Nakhon Sawan (Table 4), and three each at Kanchana Buri (Table 2) and Lop Buri (Table 3), with the values being MEI_AS (-1), MEI_DJ (-1), MEI_AS (-1), MEI_AM (-1), MEI_MJ (-1), MEI_JJ (-1) and MEI_JA (-1), respectively. SPI_NDJFMA (0) at Kanchanaburi

in Table 2 and Lop Buri in Table 3 showed that four predictors were picked out. Those were MEI_FM (-1), MEI_MA (-1), MEI_JA (-1), MEI_AS (-1) at the Kanchanaburi weather station and MEI_MA (-1), MEI_ MJ (-1), MEI_JJ (-1) and MEI_JA (-1) for the Lop Buri weather station. At Nakhon Sawan and Suphan Buri, two predictors were selected, namely MEI_FM (-1) and MEI_ AS (-1) for Nakhon Sawan, and MEI_FM (-1) and MEI_AM (-1) for Suphan Buri.

All validated results of the 3- month time scale SPI (SPI_FMA) that produced the best-fit models are graphically illustrated in Figure 5.

DISCUSSION

The results of the analysis are discussed in two main topics: the uniformity of predictor

Table 4 Predictor selection for SPI of April by step-wise method at 10% significant level and regression equations of SPI and MEI at Nakhon Sawan weather station.

SPI time scale	Start month	Regression equation
1-m	Apr (0)	SPI_Apr (0) = -0.11* MEI_ON (-1)*MEI_ND (-1) *MEI_DJ (0)
2-m	Mar (0)	SPI_MA (0) = -0.103*MEI_ON (-1)*MEI_ND (-1) *MEI_DJ (0)
3-m	Feb (0)	SPI_FMA (0) = -0.114*MEI_SO(-1)*MEI_ON (-1)*MEI_ND (-1)
4-m	Jan (0)	SPI_JFMA (0) = -0.084*MEI_AS(-1)*MEI_SO(-1)*MEI_ON (-1)
5-m	Dec (-1)	SPI_DJFMA(0) =0.352*MEI_DJ(-1)*MEI_AS(-1)
6-m	Nov(-1)	SPI_NDJFMA (0) = 0.36*MEI_FM(-1)*MEI_AS(-1)

Table 5 Predictor selection for SPI of April by step-wise method at 10% significant level and regression equations of SPI and MEI at Suphan Buri weather station.

SPI time scale	Start month	Regression equations
1-m	Apr (0)	SPI_Apr (0) = -0.076* MEI_ON (-1)*MEI_ND (-1) *MEI_DJ (0)
2-m	Mar (0)	SPI_MA (0) = -0.121*MEI_ON (-1)*MEI_ND (-1)*MEI_DJ (0)
3-m	Feb (0)	SPI_FMA(0) = -0.124*MEI_SO(-1)*MEI_ON (-1)*MEI_ND (-1)
4-m	Jan (0)	SPI_JFMA(0) = -0.097*MEI_AS(-1)*MEI_SO(-1)*MEI_ON (-1)
5-m	Dec (-1)	SPI_DJFMA(0) =-0.26*MEI_AS(-1)
6-m	Nov(-1)	SPI_NDJFMA(0) = 0.173*MEI_FM(-1)*MEI_AM(-1)

selection and the reasonable lead time forecast considering monthly MEI values issued from the download center, normally before the tenth day of each month.

The selection of predictors over the one-month to four-month time scales was more uniform than with the five- and six-month time scales. However, the lead time forecast of the five- and six-month SPI time scales was longer. This can be explained by comparing SPI_Apr (0), SPI_MA (0), SPI_FMA (0) and SPI_JFMA (0) at every station. It can be seen that the first time scale of SPI_Apr (0) provided a longer reasonable lead time forecast from the middle of February to the end of March, while the other three SPI time scales (SPI_MA (0), SPI_FMA (0) and SPI_JFMA (0))

provided a lead time forecast of one fortnight. For SPI_DJFMA (0) and SPI_NDJFMA (0), the lead time forecast was much longer than the first four-mentioned time scales, except for SPI_NDJFMA (0) at Kanchanaburi, which offered a one-fortnight forecast.

CONCLUSION

The MEI integrated complete ENSO information and therefore it might be better able to represent ENSO conditions. The MEI/SPI relationships analysis, based on the stepwise multiple regression procedure presented here showed that ENSO conditions have an impact on the insufficient seasonal rainfall during post-rainy
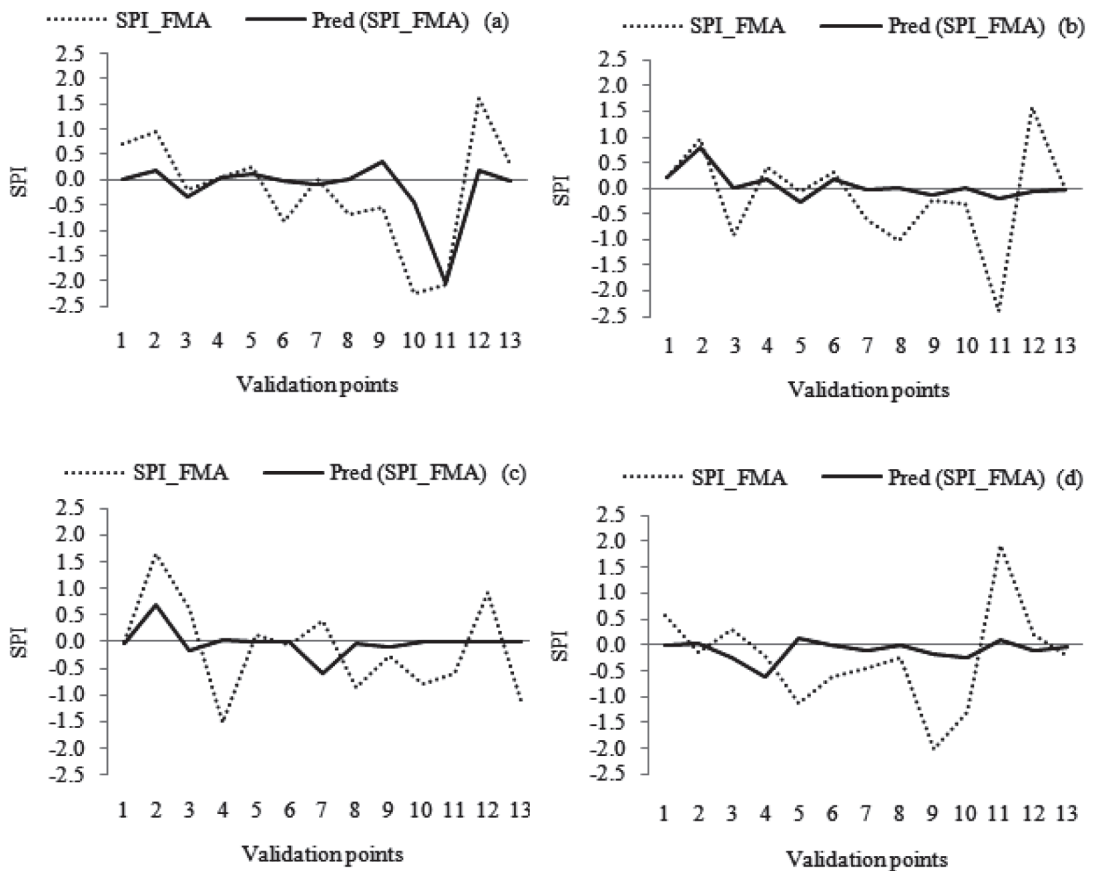

Figure 5 Validation results of 3-month time scale SPI (SPI_FMA) at (a) Kanchanaburi (b) Lop Buri (c) Nakhon Sawan and (d) Suphan Buri weather stations.

dry periods from November to April at the study sites. It can be concluded from this study that bi-monthly MEI values can provide useful indications of water resource availability. The proposed models for forecasting SPI during the dry period could contribute to irrigation water management at the paddy field level and provide useful information for the management of water resources in specific areas. For large scale management, other alternative methods might be more useful and more practicable, since this process seems to be applicable at the local rather than the global scale.

ACKNOWLEDGEMENTS

LITERATURE CITED

Bordi, I., K. Fraedrich, J.-M. Jiang and A. Sutera. 2004. Spatio-temporal variability of dry and wet periods in eastern China. **Theor. Appl. Climatol.** 79: 81-91.

Box, G.P. and G.M. Jenkins. 1976. **Time-Series Analysis, Forecasting and Control.** Holden-Day, San Francisco.

Buishand, T.A. 1982. Some methods for testing the homogeneity of rainfall records. **J. Hydrol.** 58: 11-27.

Cancelliere, A., G. Di Mauro, B. Bonaccorso and G. Rossi. 2007. Drought forecasting using the standardized precipitation index. **Water Resource Management** 21: 801-819.

Dahmen, E.R. and M.J. Hall. 1990. **Screening of Hydrological Data: Tests for Stationarity and Relative Consistency**. International Institute for Land Reclamation and Improvement / ILRI. Wageningen, The Netherlands. 54 pp.

Haan, C.T. 1977. **Statistical Methods in Hydrology.** Iowa State University Press. Ames. 378 pp.

Hanley, D., M.A. Bourassa, J.J. O'Brien, S.R. Smith and E.R. Spade. 2003. Notes and Correspondence: A Quantitative Evaluation of ENSO Indices. **J. of Climate.** 16: 1249-1258.

Hong, C.-H., K.-D. Cho and H.J. Kim. 2001. The relationship between ENSO events and sea surface temperature in the East (Japan) Sea. **Prog Oceanogr.** 49: 21-40.

Lloyd-Hughes, B. and M.A. Saunders. 2002. A drought climatology for Europe. **Int. J. Climatol.** 22: 1571-1592.

McKee, B., N.J. Doesken and J. Kleist. 1993. The relationship of drought frequency and duration to time scales, pp. 179-184. *In* **8th Conference on Applied Climatology**, Anaheim, CA.

Ortiz-Tanchez, E., W. Ebeling and K. Lanius. 2002. MEI, SOI and mid-range correlations in the onset of El Ni˜no–Southern Oscillation. **Physica A** 310: 509-520.

Otarig, C. 2000. **Assessment of El-Nino Impact on Rainfall over Thailand**. M.Sc. Thesis, Thammasat University, Bangkok.

Peskan, K.A. 2001. **A Statistical Assessment of the Relationship of the El Nino / Southern Oscillation to Great Lakes Water Levels.** MA Thesis. Windsor, Ontario.

Shabbar, A., B. Bonsal and K. Madhav. 1997. Canadian precipitation patterns associated with the southern oscillation. **J. of Climate.** 10: 3016-3027.

Singh, O.P. 2001. Multivariate ENSO Index and Indian monsoon rainfall: relationships on monthly and subdivisional scales. **Meteorol. Atmos. Phys**. 78: 1-9.

Singhrattna, N., B. Rajagopalan., K. Krishna Kumar and M. Clark. 2005. Interannual and interdecadal variability of Thailand summer monsoon season. **Am. Meteorol. Soc.** 18: 1697-1708.

Vicente-Serrano, S. 2006. Differences in spatial patterns of drought on different time scales: An analysis of the Iberian Peninsula. **Water Resour Manage.** 20: 37-60.

Wolter, K. 1999a. **Multivariate ENSO Index**. Climate Diagnostics Center. Available from: http://www.cdc.noaa.gov/ENSO.mei index.html

Wolter, K. 1999b. **Multivariate ENSO Index Data: 1950-2007**.Climate Diagnostics Center. Klaus Wolter <kew@cdc.noaa.gov.

Wolter, K. and M.S. Timlin. 1998. Measuring the strength of ENSO-how does 1997/1998 rank? **Weather.** 53: 315-324.

Wolter, K. and M.S. Timlin. 1993. Monitoring ENSO in COADS with a seasonally adjusted principal component index, pp. 52-57. *In* **Proceedings of 17th Climate Diagnostic Workshop** (Norman, Oklahoma).

Xu, Z.X., K. Takeuchi and H. Ishidaira. 2004. Correlation between El Nino-Southern Oscillation (ENSO) and precipitation in South-east Asia and Pacific region. **Hydrol. Process** 18: 107-123.